NASF SURFACE TECHNOLOGY WHITE PAPERS
88 (10), 6-26 (October 2024)

AESF Heritage:
Characterization of Deposits, Coatings and Electroforms

by
Dr. Rolf Weil, Professor Emeritus
Stevens Institute of Technology
Hoboken, NJ 07030

Editor's Note: *During the 1996-1997, the late Dr. Rolf Weil, 1981 recipient of the William Blum AESF Scientific Achievement Award, contributed a monthly column, Analytically Speaking, in the AESF journal,* Plating & Surface Finishing, *in which he described the various methods by which the properties of electrodeposits could be measured and characterized. Topics covered include analytical equipment, measurement methods and specific applications. Dr. Weil's practical approach, in layman's terms, is aimed at taking the fear out of using sophisticated equipment. What follows is a collection of several of those columns,* which still, even a quarter century later, serve as a good primer for metallurgical analysis in surface finishing.*

1. Introduction

Essentially the same methods are used to characterize electroplated, electroless, vapor deposited and chemically vapor deposited (CVD) coatings, as well as electroforms. Scanning electron microscopy is the method most frequently employed for the materials discussed here. Transmission electron microscopy and optical microscopy also have applications. The more recently developed scanning tunneling and scanning force microscopy, also known as atomic force microscopy, do not require samples to be kept in vacuum, and are therefore applicable to in-situ studies in electrolytes. Auger electron spectroscopy and X-ray photoelectron spectroscopy, or electron spectroscopy (for chemical analysis), have special uses. The characterization of the mechanical properties is important, especially for electroforms and deposits used in printed circuits. Various characterization methods, underlying principles, experimental techniques and their applications to coatings, deposits and electroforms, will be discussed.

2. X-Ray Methods

Probably the widest application of X-ray methods to deposits, coatings and electroforms is *fluorescent analysis* for the determination of chemical composition. The method is based on how X-rays are generated, which occurs when electrons or photons knock out electrons in the shells close to the nucleus of atoms. The knocked-out electrons are replaced by ones from shells farther from the nucleus. The farther electrons are from the nucleus, the greater their energy, so when an electron from a farther shell replaces one from a closer shell, the excess energy is given off as X-ray photons. The energy difference between shells is unique for any given element, and the resulting X-rays are called characteristic radiation. Because the energies or wavelengths, which are inversely proportional to the energies of the characteristic X-rays, are different for each element, they can be used to identify the element (*e.g.*, for chemical analysis). Because the characteristic X-rays are generated close to the nucleus, their wavelengths are independent of valence or the state of the material (*i.e.*, solid or liquid, elemental or compound).

Tables and computer programs are available that list the wavelengths of these characteristic X-rays for each element. The process by which knocked-out electrons are replaced by ones of higher energy (emitted as X-rays) is called *fluorescence*. When this is used to determine chemical composition, it is known as *fluorescent analysis*.

There is a system of naming the characteristic X-rays. If an electron is knocked out of the K shell, which is the one closest to the nucleus, and is replaced by one from the next-closest shell (the L shell), the X-rays are designated K_α. The letter refers to the shell of the knocked-out electron, and the subscript to the number of shells between it and the one from which the replaced electrons came. So α refers to the next-closest shell, β to the second closest, etc. If an electron is knocked out of the L shell, for example, and replaced by one from the N shell (two shells farther from the nucleus), the X-rays would be called L_β.

* Compiled and edited by Dr. James H. Lindsay, NASF Technical Editor

NASF SURFACE TECHNOLOGY WHITE PAPERS
88 (10), 6-26 (October 2024)

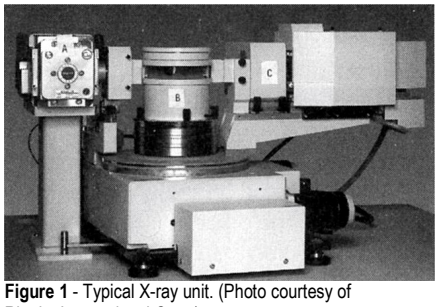

Figure 1 - Typical X-ray unit. (Photo courtesy of Rigaku International Corp.)

Typical X-ray equipment is shown in Fig. 1. For fluorescent analysis, however, it must be modified from this design. The unit consists of the X-ray tube (A), the specimen holder (B) and the counter (C). The tube contains a tungsten filament that, when heated, gives off electrons by thermal emission. The electrons are attracted to a piece of metal (the target) by applied potential.

It is important to note that electrons from the filament knock out electrons in the K shell of the target, which are replaced by ones from the L and M shells, producing K_α and K_β X-ravs. The wavelengths of the K_α and K_β radiations are characteristic of the target material (usually copper). For longer wavelengths, a chromium target is used. A molybdenum target produces X-rays of shorter wavelengths than those of copper. The potential applied between the filament and the target determines the intensity of the emitted beam. Because the filament and target are sealed in a vacuum, it is only possible to change targets by changing tubes.

As shown in Fig. 1, the position of the tube is fixed in the X-ray unit; the chamber holding the specimen rotates. As shown in Fig. 2, crystal planes parallel to the surface of the specimen make the angle θ with the emitted X-ray beam. Slits and collimators in front of the tube control the divergence of the beam, which is reflected at the angle θ by the crystal planes of the specimen parallel to its surface. The reflected beam then makes the angle 2θ with the incoming one. The counter moves on a circular track and is coupled with the rotation of the specimen. When the specimen rotates through the angle θ, the counter rotates through the angle 2θ, with respect to the incoming beam. In this way, the X-rays reflected by the surface of the specimen enter the counter. X-rays reflected by crystal planes inclined to the surface do not enter the counter when its rotation is coupled with that of the specimen. The data obtained consist of peaks (where the intensities of the X-rays entering the counter are above background) and the 2θ positions where they occur.

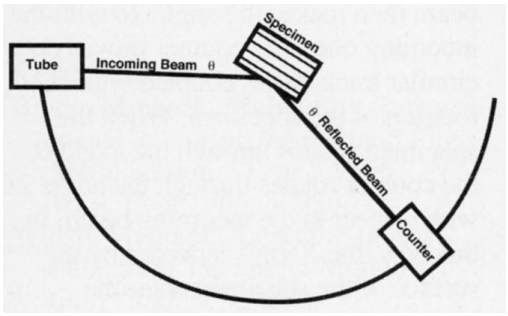

Figure 2 – Schematic of X-ray paths.

In the unit shown in Fig. 1, the track on which the counter moves is horizontal. Some units have a vertical track. Because of the reflected X-rays that do not enter the counter, it is necessary to shield the specimen. The surface of the specimen also must be at the exact center of the circular track on which the counter moves.

For fluorescent analysis, the wavelengths of the characteristic radiation produced in the sample must be determined. The conversion of the 2θ positions of the counter to wavelengths can be accomplished with Bragg's Law, which states:

$$2d \sin \theta = n\lambda \qquad (1)$$

where d is the spacing between the reflecting crystal planes, λ is the wavelength of the X-rays and θ is the angle (shown in Fig. 2). The value of n can usually be taken as unity.

Because there are three variables in Bragg's Law - d, θ and λ - it can only be solved if one of the quantities is constant and its value known. A single crystal, called the *analyzer crystal*, is placed in the specimen chamber B (Fig. 1). A lithium-fluoride crystal is often used because it can be cleaved so that a single set of planes is parallel to the surface, reflecting the X-rays into the

counter. The sample for analysis is placed in the beam path (not shown in Fig. 1). Some X-ray units can be converted for this type of chemical analysis by providing a way to place the sample in the X-ray beam. There also are units specially built for fluorescent analysis.

For fluorescent analysis, characteristic X-rays of the elements present in the sample must be produced. The X-ray photons emanating from the tube must have a definite energy or wavelength to knock out electrons from the K shell, for example, in sufficient numbers to produce peaks of relatively high intensity. It is only possible, therefore, to obtain strong characteristic X-rays from a single element. Also, the target of the tube must be selected to produce X-rays with the correct wavelength.

The fluorescent analysis method described here is called *wavelength dispersive*. The other method is called *energy dispersive*. In the wavelength dispersive method, the characteristic X-rays from the sample are reflected by the analyzer crystal into the counter at the appropriate 2θ positions. Most X-ray units have computers that convert the 2θ positions of the peaks into the wavelengths of the element's characteristic radiations present in the sample for chemical analysis and identification. With appropriate standards, the quantity of each element can be determined from the intensity of the peaks, yielding a quantitative analysis. High-intensity peaks are needed for this analysis.

Fluorescent analysis can be applied to coatings, deposits and plating solutions. It has one severe limitation - it is not possible to analyze elements of low atomic number, such as hydrogen and carbon. This can be a disadvantage if the presence of organic compounds or of gas-filled voids is to be determined in electrodeposits. The inability to analyze for boron is also a disadvantage for some electroless deposits.

The measurement of the thickness of thin foils by X-rays is based on some of the same principles as wavelength dispersive analysis and on absorption, which obeys the equation:

$$\ln \frac{I}{I_o} = -(\mu/\rho)\rho t \qquad (2)$$

where (μ/ρ) is the mass absorption coefficient listed in tables for all elements when they absorb K_α radiation. The density is ρ and the foil thickness is t. The quantities I and I_o, whose natural logarithm is substituted in Eq. (2), are obtained as follows.

A piece of metal with a small window cut out is placed in front of the tube. The counter is set at the 2θ, at which K_α-characteristic X-rays from the tube are reflected. This position is calculated from Eq. (1) by substituting the d spacing of the analyzer crystal planes, which are parallel to the surface, and the λ of the K_α radiation. This setting is necessary because the mass absorption coefficients, which vary with wavelength, are only listed for K_α radiation. The intensity of the X-rays passing through the window is I_o. When the foil is placed in front of the window, the intensity of the X-rays is I. With these two intensity measurements, as well as the density and mass absorption coefficient of the material, the thickness t can be calculated by Eq. (2).

Another phenomenon related to absorption, as well as fluorescence, is used to filter out undesirable X-rays. When X-rays emanating from the tube have the right energy to knock out electrons from the K shell, for example, in material anywhere in the path to the counter, these photons are preferentially absorbed. The wavelength at which the preferential absorption by a material occurs is called the *absorption edge*. The practical application of this phenomenon is in the production of X-rays of one wavelength (*i.e.*, monochromatic radiation). It is possible to filter out the K_β, leaving only K_α radiation, by selecting a material so that the K_β photons have just the right energy to knock out electrons in its K shell and are then preferentially absorbed. The K absorption edge of the material in the X-ray path should be just slightly longer than the wavelength of the K_β photons. The wavelength of copper K_β radiation, for example, is 0.1392 nm; the K absorption edge of nickel is 0.1488 nm. Nickel, therefore, is a suitable material to filter out K_β radiation emanating from tubes with copper targets. A thin foil of the filter material is usually placed in front of the X-ray tube.

3. Identification of Compounds

The identification of crystalline compounds or phases present in deposits, coatings or electroforms is based on a different principle than the methods for fluorescent analysis. To review, the two equations noted earlier were as follows:
Equation 1: Bragg's Law, which states:

NASF SURFACE TECHNOLOGY WHITE PAPERS
88 (10), 6-26 (October 2024)

$$2d \sin \theta = n\lambda \quad (1)$$

where d is the spacing between the reflecting crystal planes, λ is the wavelength of the X-rays and θ is the angle. The value of n can usually be taken as unity.

Equation 2: Absorption, which obeys the equation:

$$\ln \frac{I}{I_o} = -(\mu/\rho)\rho t \quad (2)$$

where (μ/ρ) is the mass absorption coefficient listed in tables for all elements when they absorb K_α radiation. The density is ρ and the foil thickness is t.

In fluorescent analysis, the d spacing of Eq. 1 was kept constant, and the variation of the wavelengths λ of the characteristic radiation with the 2θ value of the peaks was calculated. For the identification of compounds, the wavelength must be kept constant, and the variation of the λ spacing with the 2θ value of the peaks must be determined. It has been pointed out that, because of the three variables in Bragg's Law, either d or λ must be kept constant and its value known.

The identification of compounds is based on the fact that the d spacings and the relative intensities of peaks are unique for each compound or phase. To understand the method of identifying compounds, a knowledge of some basic concepts of crystallography is necessary. A crystal can be thought of as consisting of a regular three-dimensional array of points, called a *lattice*. The same pattern of one or several atoms, called the *motif* or *basis*, is associated with each lattice point. The smallest arrangement of lattice points with their associated motif is called the *unit cell*, which can be thought of as the building blocks of the crystal.

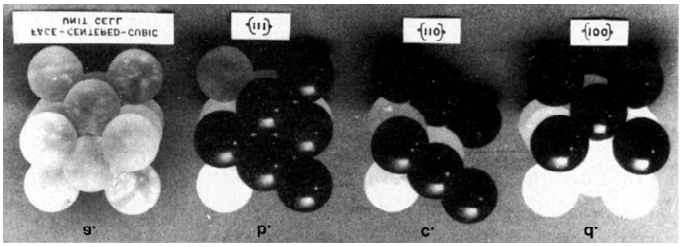

Figure 3 – Models showing the fcc unit cell (a) and family of crystal planes: (b) the {111}, (c) the {110} and (d) the {100}.

Most electroplated metals, such as copper, nickel, silver, gold and the platinum group, have the face centered cubic (fcc) unit cell shown in Fig. 3a. The motif for these metals is a single atom. There are lattice points at the eight corners and in the center of each face, each occupied by an atom in this case. The lattice points are located at the centers of the atoms. Because each corner is shared by eight unit cells, only one-eighth of the eight corner atoms is in the unit cell. Similarly, because two unit cells share a face, only half of the atoms in the six faces are in the unit cell.

The dimensions of the unit cell are called the *lattice parameters*. Iron and chromium have a body-centered-cubic (bcc) unit cell, with single atoms at the corners and one in the center. Cobalt, zinc and cadmium have a hexagonal unit cell. Many compounds (*e.g.*, sodium chloride) also have cubic lattices, so that more than one atom is associated with each lattice point. As shown in Fig. 4, the sodium ions (represented by open circles) are located

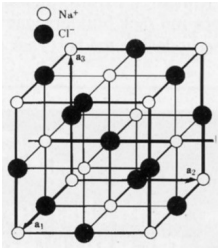

Figure 4 – Model of the sodium chloride unit cell.

on the lattice points, and the chloride ions (represented by filled-in circles) are halfway between the sodium ions, where there are no lattice points. So the motif consists of a sodium and a chloride ion.

It is convenient to name the planes in a crystal. The so-called Miller indices are named by the reciprocals of the intercepts of the crystal planes in a coordinate system in which the lattice parameters are the units of measurement. If a plane passes through the origin of the coordinate system, the origin must be moved one unit. The front face of a cube, for example, has intercepts of 1 with the Z axis, and infinity with the X and Y axes because it is parallel to them, and the reciprocals are (100). The regular brackets signify a definite plane. The (100) plane of the fcc lattice is shown by the black balls in Fig. 3d. Because all faces are identical in cubic crystals, one generally speaks of families of planes that are designated with different brackets, such as {100}. A family consists of all planes having the same three-digit indices. The face-diagonal planes are {110}, and are shown by the black balls for the fee lattice in Fig. 3c. The body diagonal planes with the indices {111} are shown by the black balls in Fig. 3b for fcc crystals. For cubic lattices, the directions that have the same three-digit indices as the planes are perpendicular to them. One direction of each of the <100>, <110> and <111> families is shown in Figs. 5a, 5b and 5c, respectively. The triangular brackets denote a family of directions (*i.e.*, all directions having the same three-digit indices).

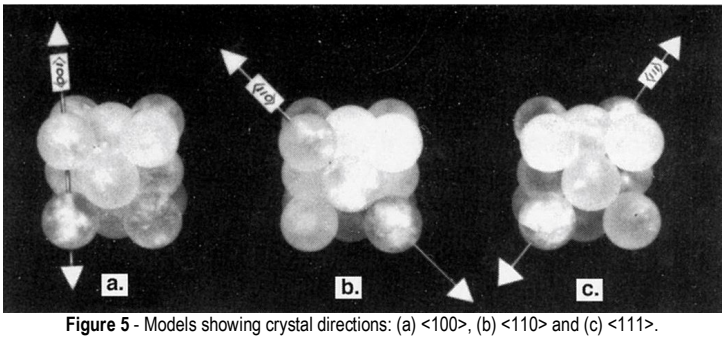

Figure 5 - Models showing crystal directions: (a) <100>, (b) <110> and (c) <111>.

As previously discussed, the identification of compounds is based on the conversion of the 2θ value, where a peak is recorded by the counter into d spacings via Bragg's Law (Eq. 1). A single wavelength, namely that of K_α, must produce the peak, and the only radiation that actually has to be eliminated is K_β. Other wavelengths are too weak to be of significance, and form the background. It was mentioned previously that a filter can eliminate the K_β radiation. Another way is to use a monochrometer, which is a curved crystal that reflects the K_β so that the peaks it produces are not recorded by the counter.

The d spacing of crystal planes depends on the lattice parameters and the Miller indices. The smaller the magnitudes of the Miller indices, the larger the d spacing. In cubic crystals, the d spacing is inversely proportional to the square root of the sum of the squares of the indices. The {100} planes, therefore, have the largest d spacing, followed by {110} and {111}. The peaks produced by {100} planes would therefore occur at the smallest 2θ position of the counter.

The intensity of a peak depends on the sum of the X-ray waves reflected by the atoms or ions in the unit cell, and on the Miller indices of the reflecting planes. The intensity also depends on a function of θ and on how many crystal planes have the same d spacing. The identification of compounds therefore requires there be the same number of all different planes parallel to the surface of the specimen, so that they can reflect X-rays into the counter. This condition can only be satisfied if the specimen consists of very small, randomly oriented crystals. Some deposits satisfy this condition; most do not, and the material must then be ground into a fine powder.

No two compounds or phases have the same value of d spacings and order of decreasing intensities. A file of approximately 30,000 X-ray patterns of crystalline materials has been compiled by the Joint Committee on Powder Diffraction Standards (JCPDS), and is available on index cards and computer diskettes. In the JCPDS file, the materials are listed first according to the values of the d spacings of the most-intense peak, and then according to the d spacings of peaks of decreasing intensity. If

NASF SURFACE TECHNOLOGY WHITE PAPERS
88 (10), 6-26 (October 2024)

the most intense peak occurred, for example, at a 2θ position of the counter that converted to a d spacing of 2.40 Å; the second to a d spacing of 1.70 Å; the third to a d of 1.45 Å; the fourth to 1.39 Å; the fifth to 1.07 Å, and the sixth to a d of 0.98 A, etc., the compound would probably be calcium oxide. It could also be another compound, such as silver scandius or rhodium tarbius. Other possibilities can readily be ruled from the chemical analysis. In most modern equipment, it is not necessary to actually perform the identification steps (*i.e.*, convert to d spacing and list them in order of intensity). Computer programs perform all the calculations, compare them to the JCPDS file, and then list the possible compounds.

The application of the above procedure would probably be only to CVD coatings, because most vapor and electrodeposits are not compounds. In some cases it may only need to be determined if a certain compound is present. An example would be annealed electroless nickel, when the presence of Ni_3P would have to be determined. In this case, the d spacings of Ni_3P would be obtained from the JCPDS file and converted to 2θ values. The presence of peaks at the values on the output of the counter would suffice to show that the deposit contained Ni_3P. The same procedure could be followed to detect the presence of oxides. The limitations of the procedure are that the compounds must be present in sufficient quantities and must be crystalline, so it is not possible to detect most organic compounds. A procedure to detect small quantities of crystalline compounds will be described later, in conjunction with electron microscopy.

4. Preferred Orientations

The preferred orientations that many deposits exhibit are generally determined by means of X-rays. Preferred orientations originate because certain crystals, which in solid materials are usually called *grains*, grow faster than others. The faster-growing grains have a certain crystallographic direction perpendicular to the substrate. This phenomenon, called *epitaxy*, occurs if the substrate is free of soils or oxides, and if the deposition rate is relatively slow. In other cases, deposition may begin with the formation of many small, randomly oriented grains (*i.e.*, having many different crystallographic orientations perpendicular to their surfaces).

In both cases, the grains having a certain crystallographic direction perpendicular to their surfaces often grow outward (away from the substrate) faster than the others. One reason why they grow faster is that some directions just naturally do so. In other instances, however, hydrogen, basic substances or the products of reactions involving addition agents are adsorbed to a lesser degree on the faster-growing grains.

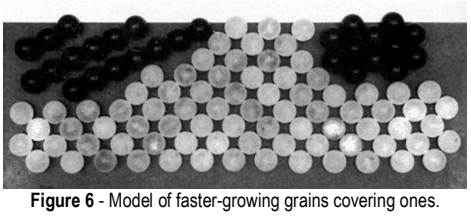

Figure 6 - Model of faster-growing grains covering ones.

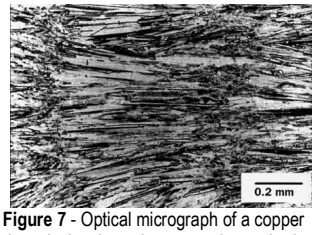

Figure 7 - Optical micrograph of a copper deposit showing columnar grains and twins.

Figure 6 illustrates that the grain represented by the white balls grew outward further than the ones shown to consist of the black balls. It is also illustrated that the faster-growing grains spread laterally, so as to cover the slower-growing ones. The faster growing grains can spread sideways until they encounter those of the same orientation. In this way, the deposit will consist mostly of grains having the faster-growing, preferred orientation. The preferentially oriented grains, by growing outward, are essentially unhindered from the columnar structure, and are often seen in the cross section of deposits (see Fig. 7).

The type of preferred orientation that results from the faster outgrowth of certain grains is called a *fiber axis* or texture, because it is similar to what is observed in a wire. In a wire, the preferred direction is parallel to its length, while in a deposit it is perpendicular to the surface. In both cases, however, the directions that are

NASF SURFACE TECHNOLOGY WHITE PAPERS
88 (10), 6-26 (October 2024)

perpendicular to the preferred one are more randomly distributed, as illustrated in Fig. 8. Here, the face of the unit cell, a plane of the {100} family is illustrated to be parallel to the surface of most grains. On the sides of the unit cells, however, the <001> directions are not parallel to each other in the different grains, and therefore more randomly distributed.

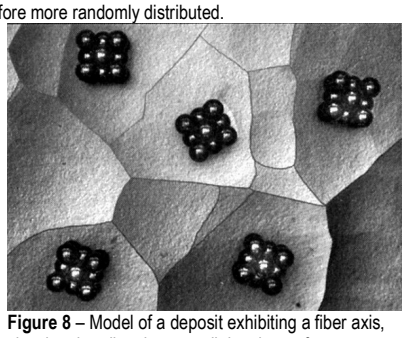

Figure 8 – Model of a deposit exhibiting a fiber axis, showing that directions parallel to the surface are random.

This randomness is characteristic of a fiber texture. A sheet texture differs in that a certain direction lying in the surface also tends to be aligned. Often this alignment occurs in the rolling direction. The determination of a fiber axis by means of X-rays is much simpler than that of a sheet texture, which involves pole figures (This will not be described further, because it requires special instrumentation and is rarely used for the materials discussed here.). A pole figure can be used to determine a fiber axis and the degree of its alignment.

The instrumentation used to determine if a fiber texture is present was shown in Fig. 1. The specimen is placed in specimen chamber B. Monochromatic K_α X-rays are directed at the specimen. A chart of intensity entering the counter vs. the (2θ) positions where peaks occur, which is called a *diffraction pattern*, is obtained. X-rays are said to diffract if the reflected beams are in phase. If a strong fiber texture is present, the intensity of certain peaks in the diffraction pattern will usually be very high. It may be recalled that the intensity is proportional to the number of grains having planes with the same interplanar spacing parallel to the surface. This number is called the *multiplicity factor*. For the identification of compounds, it was necessary that there be an equal number of grains having all the different planes parallel to their surfaces. There should be six or a multiple of six grains, for example, with a {100} plane parallel to their surfaces as there are six faces of a cube. So, for a randomly oriented sample, the multiplicity factor is six for {100} planes. The multiplicity factor for {200} planes is also six, because they are parallel to the {100} lanes. Tables of multiplicity factors for the different planes in cubic crystals can be found in most crystallography text books.

The intensities relative to the most intense peak, which is set equal to 100, of the different crystal planes of randomly oriented nickel are listed in the table at right. The relative intensities of the peaks can be calculated approximately from the product of the square of the structure factor (the sum of the X-ray waves reflected by atoms in the unit cell when a certain set of crystal planes diffracts the X-rays), the multiplicity factor and a function of (θ) called the *Lorentz polarization factor*. For face-centered-cubic crystals, the structure factor is zero, in which case there is no peak unless all the Miller indices of the diffracting planes are either all odd or all even. The number zero is considered even. There are therefore no peaks for {100} and {110} planes, because their indices are mixed.

Relative Intensities Of Diffraction Peaks of Nickel

Peak	Rel. intensity	Peak	Rel. intensity
{111}	100	{222}	7
{200}	42	{400}	4
{220}	21	{331}	14
{311}	20	{420}	15

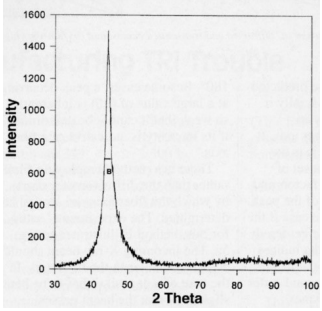

Figure 9 – Diffraction pattern of a <100> oriented nickel deposit.

According to Bragg's law (Equation 1, therefore, the smallest value of (2θ) where a peak occurs is that corresponding to the value of the interplanar spacing (d) of the {111} planes. The next peak would be that belonging to {200} planes. For body-centered-cubic crystals, the structure factor is not zero if the sum of the Miller indices is even. Again, there would not be a {100} peak. The peak with the smallest (2θ) value would be that corresponding to the (d) value of {110} peaks and the next one would again be that belonging to {200} planes, because the sums of the Miller indices are even numbers. The relative intensities, such as shown in the table, can also be obtained from the JCPDS file. It can be seen from the table that the most intense peak in randomly oriented nickel is that belonging to the {111} planes. Such is the case for most face-centered cubic metals.

If a fiber axis exists, so that most grains have a {100} plane parallel to their surfaces (as is often the case in nickel electrodeposits), there are more grains with a plane of this family parallel to the surface than predicted by the multiplicity factor. The {200} peak is then much more intense than the other peaks. As nickel is face-centered cubic, there is no {100} peak. Other peaks are much less intense than if the nickel deposit were randomly oriented, because there are fewer planes with other indices parallel to the surface. Figure 9 is a diffraction pattern belonging to a nickel deposit exhibiting a fiber texture. It can be seen that the {200} peak in Fig. 9 is much more intense than that belonging to the {111} planes. It therefore appears that relatively few grains had {311} planes parallel to their surfaces. Apparently, there were not grains with other index planes parallel to their surfaces.

When one peak is much more intense than the other ones, it is quite certain that a fiber axis exists. Then the direction with the same indices as the set of planes that caused the intense peak is the fiber axis. Many authors of technical papers have called the fiber axis of nickel <200>. The < 100> direction, however, is also perpendicular to the {200} planes. The convention is to name the fiber axis by the smallest set of indices, so even though there is no {100} peak, the fiber axis should be called <100>.

It is sometimes difficult to determine if a fiber axis exists or what its indices are. Such is the case if no very strong peak, such as that seen in Fig. 9, is observed. If the relative intensities are different from those predicted by the JCPDS file, and especially if some peaks are absent, it is an indication that there is a fiber axis. It is possible that the fiber axis is the direction perpendicular to a set of planes where the structure factor, and consequently the intensity of the peak, are zero. Such would be the case if the indices are mixed for a face-centered cubic metal or the sum of the indices is odd for a body-centered cubic one.

Then the peak of a set of second-order (indices multiplied by 2) planes, where the intensity is not zero for cubic metals, could be more intense than predicted by the JCPDS file. If the <120> direction were the fiber axis, for example, the peak belonging to {240} planes could be more intense. This method cannot always be used. The second-order peak could occur at a value of (2θ) greater than 180°. In some cases, a peak occurring at a large value of (2θ) is inherently so weak that it cannot be determined if its intensity is indicative of a fiber axis.

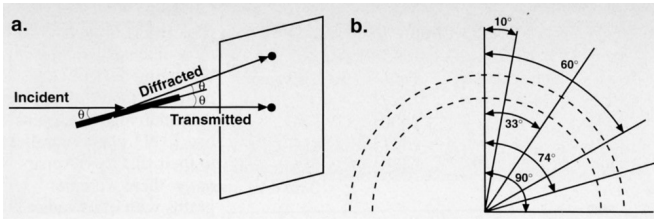

Figure 10 - Schematic representations of (a) diffracted and transmitted beams, and (b) film showing fiber axis.

There is a method employing film, rather than the diffractometer chart, by which the fiber axis can always be determined. The experimental setup for this method is illustrated in Fig. 10a. The incoming X-ray beam should be perpendicular to the fiber axis. In the case of a deposit, it has to be bent slightly so that the beam passes through the apex. The film, which is placed behind the sample (as shown in Fig. 10a), will show semicircles as illustrated in Fig. 10b. Ordinarily there would be circles, but the sample shields half of them. If a fiber axis exists, the semicircles will show small arcs of higher intensity, as illustrated in Fig. 10b. This pattern represents that of a copper deposit taken with Cu K_α X-rays of wavelength 0.542 nm. As can be seen in Fig. 10a, the distance between the spots on the film of the transmitted and diffracted beams is (D tan 2θ), where (D) is the specimen-to-film distance. The spots diffracted in different directions from the same set of planes generate the semicircle.

The inner semicircle of Fig. 10b has a radius of 2.8 cm. As D=3 cm, θ=21.5°. Because copper is face-centered cubic, the first semicircle belongs to the {111} planes. Similarly, for the outer semicircle, which has a radius of 3.6 cm and belongs to {200} planes, the value of (θ) is 25.1°. The angles between the centers of the more intense arcs and the vertical direction - designated by δ - are 33° and 74° on the {111} semicircle and 10° and 60° on the {200} one. The angles, the fiber axis and the direction perpendicular to the set of planes that produce the semicircle must be calculated by:

$$\cos \rho = \cos \theta \times \cos \delta \qquad (3)$$

where (ρ) is the calculated angle. The values of (ρ) are calculated to be 39° and 75° for the angle between the fiber axis and the <111> direction, and 27° and 63° with <100>, which, of course, is also perpendicular to <200>. From a table of angles between directions that are listed in any crystallography textbook, it is found that the angles between the <120> and the <111> directions are 39° and 75°. The angles between the <120> and <100> directions are 27° and 63°. Therefore, <120> is the fiber axis. The <120> direction also makes the angle 90° with <100>, but in most cases this higher-intensity arc is obscured by the specimen. Reflection high-energy electron diffraction (RHEED) can also be used in a way similar to the X-ray film method to determine the fiber axis. It was also previously pointed out that a pole figure can be used to determine the fiber axis.

The practical value of knowing that there is a fiber axis without actually establishing its indices is that it indicates the presence of a columnar grain structure. This fact, however, can also be established by examining the cross section metallographically. Columnar grains can be detrimental for the mechanical properties, primarily because their boundaries tend to be weak. There is essentially no effect on the mechanical properties because they depend on orientation. As was seen in Fig. 7, the directions parallel to the surface of a deposit tend to be randomly oriented when there is a fiber axis. The mechanical properties parallel to the surface - which are the important ones - therefore tend to be averaged over the different grains. Certain fiber axes are also related to the brightness of deposits.

Many technical papers erroneously list the fiber axis as the indices of the most intense peak, when they are not the smallest digits (i., <200> instead of <100>). Also, in some papers where there was a doubt about the fiber axis, the second-order peaks were not examined nor the film method applied. One purpose of this article is to prevent such errors in the future.

5. Measurement of Macrostresses

Another application of X-rays for deposits, coating and electroforms is the measurement of macrostresses. Macrostresses – often just called stresses or internal stresses - are the ones that can cause distortions of parts or cracking in chromium deposits, for example. They are referred to as macrostresses to distinguish them from microstresses.

X-rays measure the macrostresses remaining after deposition. Other methods, such as the spiral contractometer, generally measure the macrostresses during deposition and often as a function of thickness.

The macrostresses of concern in deposits are parallel to their surfaces. The spacing between the crystal planes parallel to the surface, therefore, is decreased if the macrostresses are tensile, and increased if they are compressive. According to Bragg's law, the value of (2θ) - *i.e.*, the position of the counter where a peak occurs - is changed from what it would be if there were no stresses.

If the interplanar spacing designated by (d_o) in a stress-free deposit were accurately known, the strain would be calculated from the value of (d_s), the interplanar spacing of the stressed deposit. The value of (ds) could be calculated from the (2θ) position by Bragg's law. The strain would then be $[(d_s - d_o)/d_o]$, and the macrostress would be the strain multiplied by the modulus of elasticity.

For the types of materials discussed here, however, the value of the interplanar spacing in the stress-free condition is never known with sufficient accuracy, because other factors - such as codeposited hydrogen - change it. So this simple method cannot be used for deposits.

The method that must be used is based on the fact that the strains in various directions are related by Poisson's ratio. The determination of the macrostresses is made by obtaining two (2θ) values of only one peak. One value of (2θ) is obtained from the crystal planes that are parallel to the surface of the deposit. A second value is obtained from the same planes, but inclined to the surface in other grains. The value of ($2\theta_n$) is determined with the specimen in the usual position where the rotation of the holder and the counter are coupled. Then the X-rays diffracted by crystal planes parallel to the surface enter the counter, as previously discussed.

The second value, ($2\theta_\Psi$), is obtained when the specimen holder is decoupled and rotated by the angle (Ψ), which is usually 45°, leaving the position of the counter unchanged. Then the X-rays reflected by planes inclined at the angle (Ψ) to the specimen

NASF SURFACE TECHNOLOGY WHITE PAPERS
88 (10), 6-26 (October 2024)

surface in other grains enter the counter. In order to accomplish the decoupling, a special specimen holder is required. A peak with a value of (2θ) as close to 90° should be selected for the greatest accuracy. The closer the peak is to 90°, the larger is the change of the value of (θ_n - θ_Ψ) for a given macrostress. Because peaks close to 90° generally have low intensities, an X-ray tube should be selected with a target whose value of the mass absorption coefficient of its K_α radiation for the material of the deposit is as small as possible. The macrostress (σ) can be calculated by:

$$\sigma = \frac{E \cot\ (2\theta_n - 2\theta_\Psi)}{2(1-\nu) sin^2 \Psi} \qquad (4)$$

where E is the modulus of elasticity and (ν) is Poisson's ratio. The value of the angles must be in radians.

The X-ray method is the only one that determines the macrostresses nondestructively if the part is not distorted. It is useful to study changes in the macrostress with time after plating. Many deposits exhibit such changes because of hydrogen diffusion. It is sometimes difficult to obtain an accurate value of the macrostresses by the X-ray method because, as microstresses (which are also frequently present in deposits) cause peaks to become broad. Twins cause peaks to become asymmetric. Both of these factors make it somewhat difficult to obtain an accurate value of the peak maxima, which yield the values of (2θ) used in the calculations.

6. Determining Microstrains and Particle Sizes

Another use of X-rays is the *determination of microstrains and particle sizes*. Microstrains differ from macrostrains in that they change sign - *i.e.*, from tensile to compressive over small areas of a deposit. Macrostresses have the same sign over the entire surface. The reason microstrains and particle sizes are considered together is because both cause diffraction peaks to be broadened. Particle size, determined by X-rays, is the size of regions between defects, and is generally much smaller than the grain size. Only in very fine-grained deposits are particle and grain sizes the same.

There are computer programs available for most X-ray equipment to separate the microstrain from the particle size. These programs also include the means for correcting the two other factors that cause the peaks to be broadened. One of these factors is the degree to which the X-ray beam is focused in the instrument. To determine this so-called instrumental broadening, a large-grained, well-annealed sample of the same metal is needed, or one having the same crystal structure and a similar lattice parameter can be employed.

The index of peak broadening generally used is the so-called half-width (B). It is the width of the diffraction peak in radians at half the maximum intensity, as illustrated in Fig. 11 (a duplicate of Fig. 9). The half-width of the peaks of the deposit designated by (B_d) is corrected for the half-width (B_I), because of instrumental broadening by the equation:

$$B_{st}^2 = B_d^2 - B_I^2 \qquad (5)$$

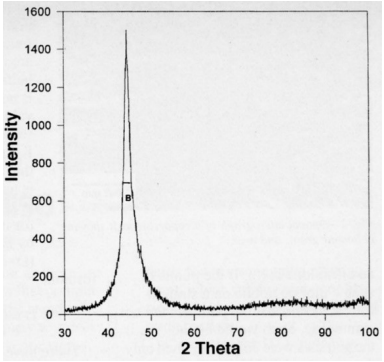

Figure 11 - Diffraction pattern of an electroless nickel deposit. Also shown is the half-width (B).

where (B_{st}^2) is the half-width of the so-called Stokes-corrected peak that is used in all subsequent calculations. The Stokes correction is usually performed by the computer program.

A second factor that can cause peaks to be broadened is that there are actually two wavelengths of K_α radiation, caused by a small difference in the energy of electrons in the L shell. There is a small energy difference, therefore, depending on which electrons in the L shell replaced knocked-out electrons in the K shell. The two different resulting wavelengths are called $K_{\alpha 1}$ and $K_{\alpha 2}$. There are also actually two peaks - one resulting from diffraction of $K_{\alpha 1}$ and one of $K_{\alpha 2}$ radiation. In most deposits, the two peaks overlap, resulting in broadening. The separation of the two peaks also increases with increasing values of (θ), so that the

NASF SURFACE TECHNOLOGY WHITE PAPERS
88 (10), 6-26 (October 2024)

broadening increases as well. It is therefore necessary to use only the half-width of the stronger $K_{\alpha 1}$ peak when calculating the microstrains and particle size. The separation of the $K_{\alpha 1}$ peak from the combined one is accomplished by what is known as the Rachinger correction. It is based on the equation:

$$I(2\theta) = I_{\alpha 1}(2\theta) + \tfrac{1}{2} I_{\alpha 1}(2\theta + \Delta 2\theta_{\alpha 1 \alpha 2}) \quad (6)$$

where [I(2θ)] is the profile - *i.e.*, the variation of the intensity with (2θ) of the Stokes-corrected peak; [$I_{\alpha 1}(2\theta)$] is the desired peak profile, only as a result of the $K_{\alpha 1}$ radiation and [$(2\theta_{\alpha 1 \alpha 2})$] is the difference in the maxima of the peaks as a result of $K_{\alpha 1}$ and $K_{\alpha 2}$. The Rachinger correction is also usually performed by the computer program.

The microstrains and particle sizes are calculated from the Stokes and Rachinger-corrected half-width (B_c). It is necessary to assume a distribution of the microstrains that can either be a Cauchy or a Gaussian one. If a Cauchy distribution is assumed, the microstrain (ε) and the particle diameter (D) are calculated by:

$$(B_c \cos\theta)\frac{1}{\lambda} = 1/D + (4\varepsilon \sin\theta)1/\lambda \quad (7)$$

Again, the computer program is generally used to calculate microstrain and particle size. The microstresses are the microstrains multiplied by the modulus of elasticity.

It is also possible to plot ($B_c \cos\theta / \lambda$) vs. ($4 \sin\theta / \lambda$) for several peaks. The intercept of the graph is then (1/D) and the slope is (ε). If the points of such a plot do not lie on a straight line, it means that the particles are not symmetric. Such would be the case if the particles were columnar. Then only the corrected half-widths of a peak, and that of a second-order one of the same set of planes, should be used in the graphs. If there is a <100> fiber axis, for example, the particle size perpendicular to the surface could be obtained by plotting the corrected half-widths of the {200} and {400} peaks.

The determination of the particle size of a powder is much simpler because there are no microstrains. The half-width of only one peak is needed. If a peak at a low value of (2θ) is selected, the separation of the $K_{\alpha 1}$ and the $K_{\alpha 2}$ peaks is very small, so that the Rachinger correction is usually not needed. The peak only has to be corrected for instrumental broadening by Eq. (5). The particle size (D) can be calculated by the formula:

$$D = 0.9\lambda / B_{st} \cos\theta \quad (8)$$

There have been relatively few studies of deposits in which microstrains and particle sizes were determined. The microstrains provide an indication of the defects that are present. Because microstrains are related to hardness, they can be used to provide a means of determining the hardness for very thin deposits where the indention method is not applicable (unless a nanohardness tester is available). The particle size can be used to determine the grain size of very fine-grained deposits.

The particle size of electroless nickel deposits decreases with the amount of the codeposited alloying element, phosphorus or boron. As the particle size decreases, the peaks become increasingly broad. Because no second-order peak is observed in Fig. 11, it is not possible to calculate the particle size and microstrain. It is likely, however, that the broadening of the peak is mostly the result of small particle size. In this case, calculating the particle size by Eq. (8), a value of ~100 nm is obtained. Because the peak was a result of diffraction from {111} planes, it is evident that there was a strong fiber axis with these planes being parallel to the surface. When the particle size approaches atomic dimensions, the deposit is considered to be no longer crystalline, but amorphous. Then only one very broad peak is observed in the intensity vs. (2θ) pattern. Such a broad peak would resemble the apparently weak one occurring between 72° and 90°.

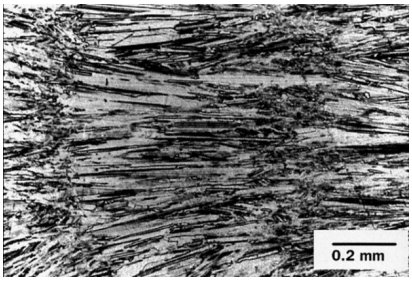

Figure 12 - Optical micrograph of a copper deposit showing columnar grains and twins.

Determination of the twinning probability is another application of X-rays. Twins are frequently observed in electrodeposits. The regions between a set of two parallel lines seen in Fig. 12 (a duplicate of Fig. 7) are twins. A twin boundary is characterized by the fact that the crystal lattice on one side is the mirror image of that on the other one. Twins are most prevalent in face-centered cubic deposits. Twin boundaries can increase the yield strength of materials in a way similar to grain boundaries, but probably to a lesser degree. The effect of twin boundaries on the strength of electrodeposits has not been investigated.

Twins affect the peaks by causing them to become asymmetric. In that case, the (2θ) value of the center of gravity (CG) of the peak - a vertical line drawn on the peaks of the diffraction pattern so that the areas on each side are equal - does not coincide with the (2θ) value, where the intensity is a maximum.

The twinning probability (*i.e.*, the ratio of the average width of twins to the size of grains) can be calculated from the asymmetry of the peak. When the deposits are face-centered cubic, the two peaks having the smallest (2θ) value on the diffraction pattern - namely, the {111} and {200 - are used in the calculation. The centers of gravity and the points of maximum intensity are determined. The twinning probability (β) can then be calculated from the difference [ΔCG(2θ)] in the value of (2θ) between the CG and the point of maximum intensity of the {111} and {200} peaks by the formula:

$$\Delta CG(2\theta)_{111} - \Delta CG(2\theta)_{200} = \beta\,[11\tan\theta_{111} + 14.6\tan\theta_{200}] \qquad (9)$$

The constants, 11 and 14.6, permit the values of (2θ) to be in degrees. If (β) is 10^{-3}, for example, and the average grain diameter is 10 μm, the twins would be 10 nm wide.

Twins can be caused by growth accidents and by mechanical deformation. The deformation-fault and growth-fault probabilities can be determined from X-ray patterns. In this case, the peak shape has to be expressed in terms of a Fourier series. The probabilities can then be calculated from the Fourier coefficients. The method is described in a paper by A.S. Fieze, R. Sard and R. Weil, which appeared in the *Journal of the Electrochemical Society*, **115**, 586 (1968).

7. The Use of Optical Microscopy

7.1 Optical Microscopy

Optical microscopes were used exclusively for the examination of the structure of deposits, coatings and electroforms until 1949. Because of the poor depth of focus of optical microscopes, one can only view the structure of polished and etched (metallographically prepared) cross sections.

"Depth of focus" is how clearly objects appear that are at various distances from the lens. Poor depth of focus can be described as when an object close to the lens appears in sharp focus, and an object in the background appears "fuzzy." The reason the as-plated surface of an electrodeposit cannot be examined with optical electron microscopy is that if protrusions appear in sharp focus, the depressions look fuzzy – or vice versa.

7.2 The Most Important Properties of Microscopes

There are three very important properties of microscopes: Depth of focus, resolution and contrast. Resolution is how closely two points or lines in the structure may be separated and still be distinguishable. The wavelength of visible light and the numerical aperture of the lens (its light-gathering ability) limit the resolution of optical microscopes. Therefore, points or lines separated less than about a micrometer cannot be distinguished.

Contrast is determined by the shades of dark and light in the image. Two points that have the same shade obviously cannot be distinguished from each other. The classic example of poor contrast is a picture of a white rabbit in the snow. In optical microscopy, contrast is primarily determined by whether structural features are inclined or parallel to the surface.

NASF SURFACE TECHNOLOGY WHITE PAPERS
88 (10), 6-26 (October 2024)

7.3 What Can Be Controlled

The three aspects of microscopes that can be controlled are the magnification, the illumination and the focus. The magnification of optical microscopes is determined by the product of the magnifying power of two lenses and the effective distance between them. The two lenses are the objective lens and the eyepiece. For metallographs that are optical microscopes with attachments for photographing the structure, the distance between the eyepiece and the camera also determine the magnification.

Optical microscopes, as the name implies, use visible light for observing the structure. Most also have means for polarizing the light or tinting it. Polarized and tinted light can aid in the identification of non-metallic inclusions. Focusing primarily is accomplished by changing the distance between the specimen surface and the objective lens. For objective lenses of high magnifying power, this distance is so short in air that the lens touches the specimen surface. By immersing the lens in a drop of oil, the numerical aperture is changed so that the distance-to-focus between the specimen surface and the lens is lengthened.

Contrast is determined by whether structural features are parallel to the surface or inclined. Microscopes are generally operated in the so-called "bright field mode." In this mode, the light reflected by structural features perpendicular to the incoming light beam is reflected back into the objective lens and the features therefore appear bright. Features inclined to the incoming light beam reflect it outside the lens, and therefore appear darker.

To attain contrast, some portions of structure must be inclined to the incoming beam. The main purpose of etching (attacking the specimen, usually with an acid) is to attain contrast. A polished surface would not exhibit contrast because it wholly reflects the light into the objective lens and therefore appears uniformly bright. By etching, some structural features become inclined to the beam and, as a result, appear darker. In this way, the grain structure can be distinguished. Through the use of certain etchants, grains are attacked differently, depending on which crystal plane is parallel to their surfaces. Different grains exhibit various shades of light and dark.

The as-plated surfaces of deposits that are not fully bright generally show structural features that are inclined and therefore do not require etching. As was previously discussed, the whole surface would not be in focus. Some inclined features may look like grain boundaries. They are often the crevices surrounding nodules, however. Even if the depth of focus permits being able to observe the structure, the grain size should not be determined from observations of the as-plated surfaces of deposits. The cross sections of deposits need to be polished and then etched. Polishing a specimen, especially a relatively soft metal, can result in severe plastic deformation. This plastically deformed layer must be removed by repeated etching and slight repolishing or it will obscure the true structure.

8. The Use of Scanning Electron Microscopy (SEM)

The main advantages of scanning electron microscopy (SEM) over optical ones are better resolution and depth of focus. The superior depth of focus of the SEM permits the examination of rough surfaces, such as fractures. Even such rough surfaces as dull electrodeposits would be wholly in focus. Because it is often difficult to distinguish crevices surrounding nodules from the boundaries of grains, great care must be exercised if their size is to be determined by SEM.

8.1 Advantages & Disadvantages

Figure 13 shows a scanning electron micrograph of electroless nickel. It illustrates that the features resembling grains are, in fact, nodules. Even if there are structural features - such as the lines seen in Fig. 13 that appear to extend across grains - it is still difficult to determine the actual grain size. It is best, therefore, not to determine the grain size of deposits by SEM.

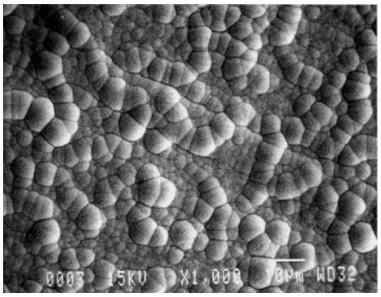

Figure 13 – Scanning electron micrograph of electroless nickel, showing nodules often mistaken for grains.

The principal disadvantage of the SEM is that the samples are in a vacuum. In situ observations of electrodeposition or corrosion cannot be made. Such observations are possible by optical microscopy. The surfaces of non-metallic materials have to be coated with a very thin film of a conducting material, usually gold. Otherwise, charges develop that can obscure the structure.

Recently developed scanning electron microscopes, in which the electrons are produced by field emission, permit the use of low accelerating voltages. A scanning electron microscope, however, is much more expensive than an optical microscope.

8.2 Operation of the SEM

As implied by the name, the SEM uses electrons rather than visible light for illumination. The wavelength of electrons is several orders of magnitude smaller than that of photons in the visible range. The resolution, therefore, is not limited by the wavelength, and the quality of the lenses determines the resolution. For the examination of most deposits, the resolution of an SEM is adequate.

Contrast is determined by the mode in which the SEM is operated. The two main modes use back-scattered and secondary electrons, respectively. In the back-scattering mode, the incoming electrons are reflected by the surface of the specimen. Contrast is achieved primarily by how much energy the electrons lose when they are reflected. The smaller the atoms that reflect them, the more energy the electrons lose. As an analogy, when a ping-pong ball hits a bowling ball, it does not lose any energy - it only changes direction. It cannot transfer any energy to the bowling ball because it cannot move the bowling ball. If a ping-pong ball hits a tennis ball, however, the latter is moved a little, so the former loses energy.

If only back-scattered electrons with energies greater than a certain value are imaged, structural features consisting of small atoms will appear darker than those consisting of mostly large atoms. The reason for the contrast, therefore, is that only the electrons back-scattered by the large atoms are imaged. An example would be annealed electroless nickel containing Ni_3P particles. Because the phosphorus atoms are smaller than the nickel atoms, the Ni_3P particles would appear darker than the nickel matrix. So if the desired contrast depends on atomic weight, the SEM should be operated in the back-scattering mode.

In most cases, the morphology (*i.e.*, the protrusions and depressions) needs to be viewed, so secondary electrons should be imaged. When an electron scans a specimen in the SEM, other electrons are emitted. These secondary electrons are much less energetic than the ones that cause them to be emitted. So only those secondary electrons emitted near the surface cannot escape out of the material and be imaged. The closer to the surface the secondary electrons are emitted, the brighter the image.

The contrast depends, therefore, on the length of the path to the surface. The greater the path length, the fewer secondary electrons are imaged and the darker the region appears. The path length of an inclined structural feature, for example, is greater than that of one that is parallel to the surface. Figures 13 and 14 were both produced in the secondary-electron mode.

Most SEMs are equipped with a means to perform chemical analysis. Essentially, in this method, the electrons knock out other ones in the lower shells of the atoms. When electrons from shells farther from the nucleus take their place, the energy difference is emitted as characteristic X-rays.

The elements present in a sample can be identified from the wavelengths of their characteristic X-rays. The main difference between a fluorescent-analysis method and that attached to an SEM lies in the size of the area that can be analyzed. Because the electron beam in an SEM can be focused on a small area of the specimen, it is possible to chemically analyze very small structural features, such as a small codeposited particle. The

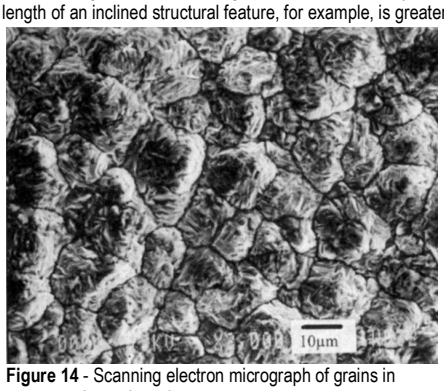

Figure 14 - Scanning electron micrograph of grains in a copper electrodeposit.

NASF SURFACE TECHNOLOGY WHITE PAPERS
88 (10), 6-26 (October 2024)

limitation of the fluorescence method - the inability to analyze elements of low atomic number, such as hydrogen – also applies to the SEM attachment.

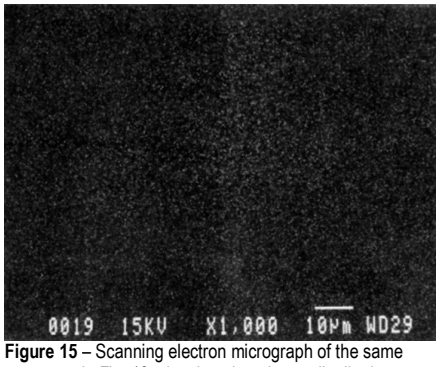

Figure 15 – Scanning electron micrograph of the same area seen in Fig. 13, showing phosphorus distribution.

The characteristic X-rays can also be imaged in the SEM. It is therefore possible to determine how a given element is distributed. In Fig. 15, which represents the same areas as that shown in Fig. 13, characteristic X-rays of phosphorus were imaged. By careful analysis, it may be seen that the crevices in Fig. 13 contain more phosphorus than other areas. A disadvantage of the SEM is that it is not possible to obtain regular diffraction patterns. It is therefore not possible to determine crystallographic information, such as the directions of the fine lines in Fig. 14 or the orientation of a given grain. It is possible to obtain a type of diffraction pattern - called a bitter pattern - from large grains, but these patterns are very difficult to obtain and to interpret.

9. The Use of Transmission Electron Microscopy (TEM)

Transmission electron microscopy (TEM) differs from scanning electron microscopy (SEM) in that the electrons pass through the specimen. The main disadvantage of TEM, therefore, lies in specimen preparation. The specimen must be a thin foil, about 100 nm thick, in order for the electrons to be transmitted. Thicker specimens must be thinned either by electropolishing or ion milling.

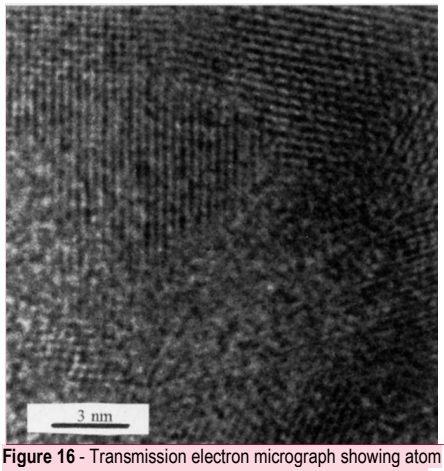

Figure 16 - Transmission electron micrograph showing atom rows in a crystal of yttrium oxide. (Photograph provided by J. Taylor of Stevens Institute.)

Advantages of TEM over SEM are better resolution and the ability to obtain diffraction patterns. The principal uses of TEM for deposits, coatings and electroforms are determination of the sizes and orientations of the grains, and the density and distribution of structural defects. The resolution of the TEM is high enough to image the atomic structure. Figure 16 shows the images of atoms and crystal planes in a sample of yttrium oxide. The planes of atoms are ~3 Å apart. The changes in the orientation of the planes of atoms in different tiny grains is clearly seen.

The contrast in the TEM of crystalline materials is primarily determined by the degree to which Bragg's law is obeyed. The electrons either pass through the specimen - *i.e.*, they are transmitted or diffracted if crystal planes are oriented in a particular area so that Bragg's law is obeyed. An aperture is placed below the specimen in such a way that either the transmitted beam or a diffracted one is allowed to pass through. If the transmitted beam passes through the aperture, the image is said to be a bright-field one. If a diffracted beam passes through the aperture, a so-called dark-field image results. In a bright-field image, therefore, in areas where Bragg's law is not obeyed, the electrons constitute the transmitted beam and can pass through the aperture. The image of this area therefore appears bright. Where there are crystal planes oriented for diffraction, the electrons are the diffracted beam that cannot pass through the aperture, so this area appears dark in the bright-field image. The opposite applies to a dark-field image.

Commented [JL2R1]:

Commented [JL3]:

Commented [JL1]:

NASF SURFACE TECHNOLOGY WHITE PAPERS
88 (10), 6-26 (October 2024)

9.1 Bend Fringes & Thickness Fringes

Figure 17 is a bright-field TEM of electrodeposited nickel, showing many of the structural features observed in this material. The area marked "A" is dark because crystal planes are oriented so as to obey Bragg's Law. The electrons emanating from this area are diffracted and cannot pass through the aperture. If the aperture were placed to allow the diffracted electron to pass through, area A would appear light. The dark band in the area marked "D" is called a bend fringe. Because the specimen is very thin, it sags a little, and the crystal planes, therefore, are not exactly parallel. In the dark band, the crystal planes obey Bragg's law so that the electrons are in a diffracted beam, which again cannot pass through the aperture. Bend fringes can be easily identified because they move if the specimen is tilted. The ability to tilt the specimen is a feature of every TEM, so that any area can become oriented for diffraction. Bend fringes have no practical application.

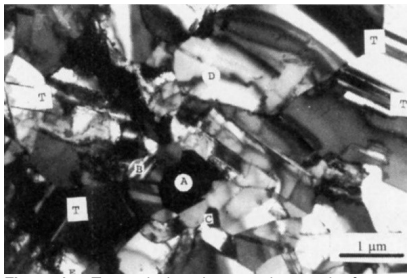

Figure 17 - Transmission electron micrograph of a nickel electrodeposit.

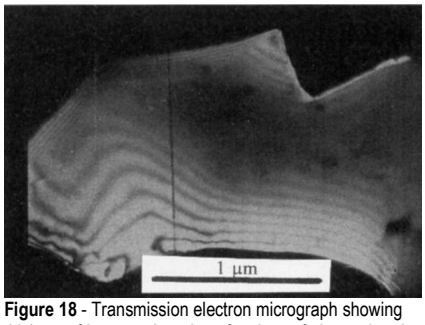

Figure 18 - Transmission electron micrograph showing thickness fringes at the edge of a piece of electroplated nickel.

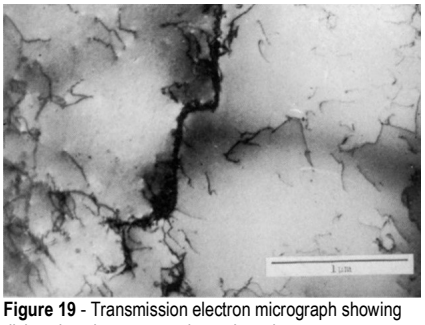

Figure 19 - Transmission electron micrograph showing dislocations in a copper electrodeposit.

Thickness fringes appear at area "C" in Fig. 17, although they are difficult to distinguish because they are very close together. Figure 18 shows them more clearly. Thickness fringes are sets of parallel, alternate dark and light bands. They are also parallel to an edge of a hole where the specimen is wedge-shaped, or to an inclined grain boundary, as in Fig. 17. Thickness fringes can be used to estimate the thickness of the specimen.

9.2 Dislocations & Twins

The two structural defects most commonly observed in deposits, coatings and electroforms are also seen in Fig. 17. Dislocations that greatly affect the mechanical properties are shown in the area labeled "E." They are the fine, dark lines. Figure 19 shows dislocations at higher dislocations form a low-angle grain boundary when they pile up. The dislocations can resemble the bend fringes seen in area D of Fig. 17. Dislocations can be readily distinguished from bend fringes, however, because they do not move when the specimen is tilted. The bands bounded by a set of parallel lines are shown in the area marked "B" in Fig. 17. They may contain sets of parallel lines, or they may not be seen, such as in the areas marked "T." Twins are caused by accidents during crystal growth, and tend to have a strengthening effect.

NASF SURFACE TECHNOLOGY WHITE PAPERS
88 (10), 6-26 (October 2024)

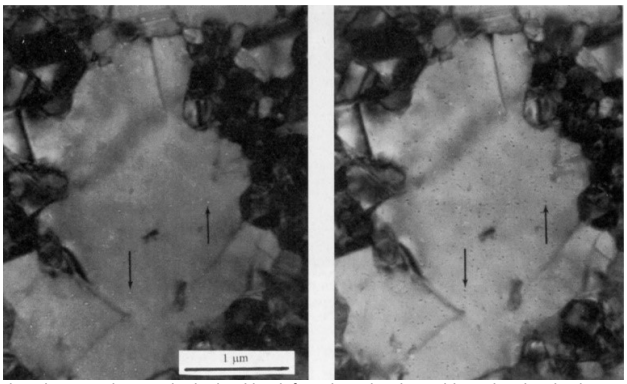

Figure 20 - Transmission electron micrograph obtained by defocusing, showing voids and molecules in a cobalt-hardened gold electrodeposit. (Photograph provided by Dr. Nakahara of Lucent Technologies.)

An application of the TEM that is uniquely suited to electrodeposits is the ability to observe tiny voids and inclusions of organic molecules. The molecules are generally the addition agents or their reaction products. The voids and molecules are made visible by slightly defocusing the image. Electrons travel faster through molecules composed of atoms of low atomic weight or the empty space of voids, than through the heavier metal. The objective lens normally combines the electron waves traveling at different velocities. However, by slightly defocusing the image so that the electron waves are not combined, the voids and molecules become visible. Figure 20 shows the structure of a cobalt-hardened gold deposit that exhibits the so-called polymer inclusions. The inclusions appear as small dots, several of which are indicated by arrows. In Fig. 20a, the dots appear lighter than the background; in Fig. 20b, the same dots are darker than the background. The dots change from dark to light as focus is passed. Figure 20a was overfocused by 3.9 μm, while Fig. 20b was underfocused by the same amount.

9.3 The Use of TEM for Determining Grain Size

Probably the widest application of the TEM to coatings, deposits and electroforms is in the determination of grain size. This procedure involves electron diffraction. The magnification is reduced so that the electron beams diffracted by the various sets of crystal planes in one grain become points in a photograph. An electron diffraction pattern of a single grain in a nickel electrodeposit is shown in Fig. 21. The angle between the transmitted and a diffracted beam is 2θ. In Fig. 21, the spot caused by the transmitted beam is the most intense, and is labeled No. 1. It is considered the origin and becomes the [000] beam. Spots caused by diffracted beams are labeled with the other numbers. From a diffraction pattern such as that shown in Fig. 21, it is possible to determine the Miller indices of the crystal plane, which was perpendicular to the incident electron beam, as well as crystallographic directions in the plane. For the indexing procedure, Equation (1) is used:

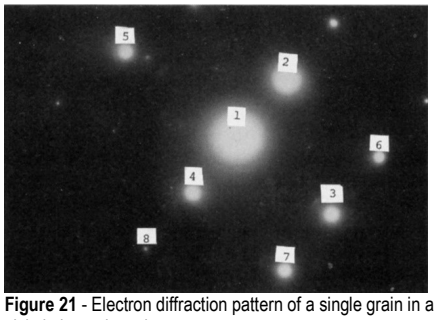

Figure 21 - Electron diffraction pattern of a single grain in a nickel electrodeposit.

$$h^2 + k^2 + l^2 = (Ra_oK)^2 \qquad (10)$$

where *h*, *k* and *l* are the Miller indices of the planes that produced the spot, *R* is the distance between the origin and the spots caused by diffracted beams, a_o is the lattice parameter of the material, and *K* is a constant. The way to calculate K will be discussed later. The magnitude of *R* and the direction from the origin to a spot is a vector. The three indices of the vector, [*hkl*], are its components in the X, Y and Z directions of the coordinate system.

The indexing method consists of measuring the distance between the centers of the spots caused by the transmitted beam and the two nearest diffracted beams. The No. 2 spot is the one caused by the diffracted beam that is nearest to spot No. 1 (the origin). The distance between No. 2 and No. 1 is ~ 2.5 cm. The value of K is 1.966×10^7 cm^{-1} and a_o of nickel is 3.5239×10^{-8} cm. Therefore, by Eq. (1):

$$(h^2 + k^2 + l^2) = (2.5 \times 1.966 \times 107 \times 3.5239 \times 10^{-8})^2 \approx 3$$

Nickel has a face-centered cubic crystal structure, so the sum of the squares of the Miller indices of the planes that produced spot No. 2 are of the {111} family, because the sum of the squares is 3. Because the Miller indices are digits, calculating the sum of their squares by Eq. (1) beyond the decimal point has no meaning. The distance between spot No. 1 and No. 3, the next-nearest one, was 4.1 cm. If this value of R is substituted into Eq. (1), then $(h^2 + k^2 + l^2)$ equals about 8. The Miller indices of the planes that produced spot No. 3, therefore, are of the {220} family.

10. Auger Electron Spectroscopy

Auger electron spectroscopy (AES) is used mainly to obtain a chemical analysis of essentially the top layers of atoms that constitute the surface. To understand Auger electron spectroscopy, it is first necessary to review the production of characteristic X-rays, which was discussed in Section 2 of this paper. It may be recalled that characteristic X-rays are produced when an electron knocks out another one in the levels close to the nucleus, such as the K shell. The vacancy is then filled by an electron from the L shell, for example, which has a higher energy. The energy difference can then be emitted as X-ray photons. In this case, the radiation is called K_α. It was previously discussed in conjunction with microstrain and particle size measurements, that there are two slightly different wavelengths of K_α radiation, namely $K_{\alpha 1}$ and $K_{\alpha 2}$. The reason for two wavelengths of K radiation is that there are three energy levels in the L shell. They are designated as L_I, L_{II} and L_{III}. When an electron from the L_{III} level fills the vacancy in the K shell, $K_{\alpha 1}$ X-rays result. If the electron filling the vacancy in the K shell originated in the L_{II} level, the resulting radiation is $K_{\alpha 2}$.

A process other than production of characteristic X-rays, such as K_α, can take place, especially in elements with atomic numbers less than 31, which is gallium. If a vacancy in the K shell, for example, is filled by an electron from the L_I level, the resulting $K_{\alpha 2}$ radiation may not escape from the atom. Instead, an electron is ejected from the L_{III} level, for example. This electron is called an Auger electron and it has an energy or wavelength characteristic of the energy difference between the K and L shells. This energy difference is unique to each element and can, therefore, be used to identify it.

The energy of Auger electrons is very small. Consequently, they are absorbed by the material being tested, except for the very top layers of atoms in the surface. In this way, the surface can be chemically analyzed, as only Auger electrons from it can escape. The principal application of Auger electron spectroscopy is, accordingly, chemical analysis of the surface layer. The various energies of the emitted Auger electrons result in peaks that can be identified, resulting in a qualitative analysis.

There are related applications of AES. A quantitative analysis can be obtained from the intensity of the AES peaks with suitable standards. A depth profile can be achieved by sputtering off successive surface layers by inert ion bombardment and determining the composition of each one by AES. The uniformity of layer removal by sputtering limits the depth resolution. A depth profile can also be obtained by polishing a cross section of the deposit at a shallow slant. In this way, the area of a layer is greatly increased. Because electrons can be focused, a very small area can be analyzed. This capability can be applied to the newly created surface of each layer. Small shifts in the wavelength of the peaks can provide information about the oxidation state or valence of the elements, and so indicate whether they exist in compounds. For example, aluminum has an Auger peak at 68 eV. The peak of aluminum in Al_2O_3 occurs at 51 eV. It is then possible to differentiate between elemental aluminum and its being combined in the oxide. There should be no other elements present with peaks near the ones in question. As will be discussed in the next section, X-ray photoelectron spectroscopy (XPS) is more suitable for the determination of specific compounds.

There are some problems and limitations associated with AES. Insulating materials can present problems in that they can develop a charge. This problem is especially acute if the surface is not smooth. It is best to limit the AES analysis to conducting

materials. Hydrogen and helium cannot be analyzed because they do not have L shells. The low energy of the Auger electrons can cause them to be absorbed by air molecules; an ultra-high vacuum is therefore required.

11. X-ray Photoelectron Spectroscopy

X-ray photoelectron spectroscopy (XPS), also known as electron spectroscopy for chemical analysis (ESCA), provides information about compounds in the surface layer. It involves electrons being knocked out of their shells. It was previously discussed that fluorescent analysis is also based on X-ray photons knocking out electrons in the lower shells of atoms and having electrons from shells of higher energy filling the vacancies. The difference in energy is given off as characteristic X-rays. Because this energy is different for each element, a chemical analysis can be made. The electron that is knocked out of the shells, creating a vacancy, is called a photoelectron. The energy of photoelectrons is weak, so that they can escape only from the near-surface layer.

XPS provides a means of determining the binding energy of the atoms in the surface layer. High energy X-rays should be used to produce the photoelectrons. It is preferable to use monochromatic X-rays. In this way, satellite peaks are avoided. The binding energy of an electron in the shell from which it came can be calculated, knowing the energy of the X-ray source and the kinetic energy of the photoelectrons. A constant, such as the work function of the spectrometer, must also be determined independently. The binding energy is the difference between the energy of the X-ray source and the sum of the kinetic energy of the photoelectrons and the constant. The binding energies provide information about the elements present in the surface layer and whether they are present in the elemental state or as compounds. Identification of the elements or compounds present can be made by comparison of the peaks with data compiled in the literature. The detection limits vary from 0.1 to 1 atomic percent, which is comparable to AES.

An advantage of XPS over AES is that more precise information about the compounds present is provided. This information is obtained from shifts of the peaks. Another advantage over AES is that it can be readily used for insulating materials. The X-rays used for XPS do not cause a charge build-up in the way electrons do when they are not conducted away. Depth profiling can be carried out by sputtering off layers or with tapered sections in the same way as with AES. Because X-rays cannot be focused in the same way as electrons, however, AES can analyze a smaller area than can XPS. A larger database exists for the interpretation of XPS data than for AES. The two methods are often used together; if a precise value of the binding energy cannot be readily obtained, AES data can help.

12. Secondary Ion Mass Spectroscopy

Secondary ion mass spectroscopy (SIMS) is used primarily for measurements of depth penetration. It is essentially a gas analysis. Layers are sputtered off the sample by a monoenergetic ion beam. Charged particles come off the surface as a result of the ion bombardment. Before they can be redeposited, they constitute a gas that can be analyzed by a mass spectrometer.

In most applications, the primary ion beam has energies ranging from 0.5 to 50 keV and is rastered over the sample surface. If the rate of material removal is known, data about depth profiling can be obtained from the gas analysis. The technique is very sensitive for detection of small impurities in the range of parts per million. It is particularly useful in the study of semiconductor materials. With suitable standards, the method can be made quantitative. If information about surface contaminants is desired, a low ion flux is employed so that only part of the top layer of molecules is sputtered off.

13. Low Energy Electron Diffraction

Low energy electron diffraction (LEED) provides information about the crystal structure of the surface layer. The arrangement of atoms (*i.e.*, the crystal structure in the surface layer) is different from that in the bulk of the material. The main reason for this difference is that the number of nearest neighbors is not the same. Also foreign species, such as oxygen, are more prevalent in the surface layer.

NASF SURFACE TECHNOLOGY WHITE PAPERS
88 (10), 6-26 (October 2024)

Determination of the crystal structure was discussed previously. If an electron beam of low energy, on the order of 5 keV, is diffracted by the surface layer, its crystal structure can be determined. Interpretation of the diffraction patterns is easier if the pattern of a single crystal is obtained.

Most transmission electron microscopes are not equipped to perform LEED unless they have a special chamber for it. For this technique, the electron beam is almost parallel to the surface. In the TEM for selected-area diffraction, as previously described, the electron beam is perpendicular to the specimen surface. Most work with LEED is performed in a special instrument that can also be used for high-energy electron diffraction.

14. About the Author

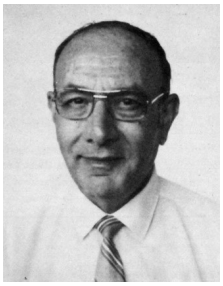

Dr. Rolf Weil was born in Neunkirchen, Germany, he came to the U.S. in 1940. He attended Carnegie Institute of Technology in Pittsburgh and received B.S. and M.S. degrees in metallurgy in 1946 and 1949, respectively. During this period he was employed as a metallurgist at Duquesne Smelting Corp.

He began work toward his Ph.D. in 1949 as a graduate assistant to Prof. Harold Read at the Pennsylvania State University. His doctoral thesis, accepted in 1951, was the first study of electrodeposition using electron microscopy. He then worked as a metallurgist at Argonne National Laboratory and Picatinny Arsenal. After two years of service in the Army, Dr. Weil joined Stevens Institute of Technology in Hoboken, NJ, as an assistant professor. He continued the research started at Penn State, became an Associate Professor in 1961, and was named Full Professor in 1967.

His work led to the establishment of a highly successful research program for electrodeposition at Stevens Institute. At the time, few universities had such an active program in this area. Under his direction, numerous students have received M.S. and/or Ph.D. degrees. Many of his associates have been employed by industrial laboratories and continue to make valuable contributions to the advancement of the finishing industry.

One of Dr. Weil's most significant achievements was his explanation of how the structures of electrodeposited metals develop, and how structure is related to the properties of a deposit. As a metallurgist, Dr. Weil approached this question from the perspective of analyzing the deposit rather than the chemical composition of baths. Using electron microscopy, he was able to resolve the grain structure of bright nickel deposits, and formulated the first theory relating surface morphology and brightness.

Early in his career, Dr. Weil noted the effects of sulfur-containing brighteners on the corrosion of nickel, a relationship important to the development of duplex nickel coatings. Other research defined the structure of the palladium-tin activator used for electroless plating and revealed how an electroless deposit was formed on activated sites.

Equally valuable have been Dr. Weil's publications about the origin and measurement of internal macro- at micro-stress, and in this area he was a leading authority. His observations also explained why deposits have a high density of dislocations, resulting in hardness and low ductility.

In all his years of research, Dr. Weil authored numerous technical articles, and he was asked to write the treatises on electroless and electrolytic plating for the Encyclopedia of Science and Technology. He was co-author with Dr. Read of the chapter "Metallurgical Principles" in Modern Electroplating, and was co-editor of The Proceedings of the Symposium on Electrocrystallization presented by the Electrochemical Society in 1981. He also served on the Editorial Board of Surface Technology.

Dr. Weil was honored as the first recipient of the Research Award of the Electrodeposition Division of the Electrochemical Society in 1979. In addition to his outstanding research contributions to the field of electrodeposition, he was cited as being instrumental in the organization of annual conferences on this topic at Penn State.

Dr. Weil enjoyed a long and prosperous relationship with the AES/AESF, and shared his knowledge in presentations for members of the society's Newark, Detroit, and Boston Branches. In 1970, he received the John J. Hanney Memorial Award for the best paper on copper plating presented at the annual conference, and he presented numerous papers at AES/AESF symposia in recent years. He served as Director of AES/AESF Research Projects 22, 30 and 38, and prepared an Illustrated Lecture to explain in simplified terms the results of this research on structure/property relationships of electrodeposits.

Dr. Weil was named the recipient of the 1981 AES Scientific Achievement Award at the 68th AES Annual Technical Conference in Boston. He has received international recognition for many years for his scientific discoveries in the field of electrodeposition.